Spatiotemporal dynamics of 5-HT6 receptor ciliary localization during mouse brain development

Vincent Dupuy, Matthieu Prieur, Anne Pizzoccaro, Clara Margarido, Emmanuel Valjent, Joël Bockaert, Tristan Bouschet, Philippe Marin, Séverine Chaumont-Dubel

Neurobiology of Disease 176 (2023) 105949

Contents lists available at ScienceDirect

Neurobiology of Disease

journal homepage: www.elsevier.com/locate/ynbdi

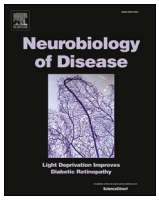

Spatiotemporal dynamics of 5-HT$_6$ receptor ciliary localization during mouse brain development

Vincent Dupuy, Matthieu Prieur, Anne Pizzoccaro, Clara Margarido, Emmanuel Valjent, Joël Bockaert, Tristan Bouschet, Philippe Marin [1], Séverine Chaumont-Dubel [*,1]

Institut de Génomique Fonctionnelle, Université de Montpellier, CNRS, INSERM, Montpellier, France

ARTICLE INFO

Keywords:
Serotonin receptor
Primary cilium
Neuronal development

ABSTRACT

The serotonin 5-HT$_6$ receptor (5-HT$_6$R) is a promising target to improve cognitive symptoms of psychiatric diseases of neurodevelopmental origin, such as autism spectrum disorders and schizophrenia. However, its expression and localization at different stages of brain development remain largely unknown, due to the lack of specific antibodies to detect endogenous 5-HT$_6$R. Here, we used transgenic mice expressing a GFP-tagged 5-HT$_6$R under the control of its endogenous promoter (Knock-in) as well as embryonic stem cells expressing the GFP-tagged receptor to extensively characterize its expression at cellular and subcellular levels during development. We show that the receptor is already expressed at E13.5 in the cortex, the striatum, the ventricular zone, and to a lesser extent the subventricular zone. In adulthood, it is preferentially found in projection neurons of the hippocampus and cerebral cortex, in striatal medium-sized spiny neurons, as well as in a large proportion of astrocytes, while it is expressed in a minor population of interneurons. Whereas the receptor is almost exclusively detected in the primary cilia of neurons at embryonic and adult stages and in differentiated stem cells, it is located in the somatodendritic compartment of neurons from some brain regions at the neonatal stage and in the soma of undifferentiated stem cells. Finally, knocking-out the receptor induces a shortening of the primary cilium, suggesting that it plays a role in its function. This study provides the first global picture of 5-HT$_6$R expression pattern in the mouse brain at different developmental stages. It reveals dynamic changes in receptor localization in neurons at the neonatal stage, which might underlie its key role in neuronal differentiation and psychiatric disorders of neurodevelopmental origin.

1. Introduction

The formation of neuronal circuitry is a complex and highly regulated process. Even slight alterations of this process can lead to the appearance of neurodevelopmental pathologies. Besides neurotrophins, certain neurotransmitters are key regulators of neurodevelopmental processes, such as neuronal differentiation, migration, dendritic morphogenesis, synaptogenesis and adult neurogenesis (Cai et al., 2021; Daubert and Condron, 2010; Deneris and Gaspar, 2018; Tang et al., 2021). Serotonin (5-HT) is one of the first neurotransmitters for which a developmental role was established using either pharmacological tools or knockout mouse models(Gaspar et al., 2003).

5-HT exerts its effects through the activation of many receptor subtypes (14 subtypes identified in humans). Except for 5-HT$_3$ receptors, all 5-HT receptor subtypes belong to the G protein-coupled receptor (GPCR) family. Of these, the 5-HT$_6$ receptor (5-HT$_6$R) is a Gs-coupled receptor that has emerged as a key player in several neurodevelopmental processes (Dayer et al., 2015; Duhr et al., 2014; Jacobshagen et al., 2014; Pujol et al., 2020). The 5-HT$_6$R interacts with and activates Cyclin-dependent kinase (Cdk)5 to promote the migration of cortical pyramidal neurons (Dayer et al., 2015; Jacobshagen et al., 2014). The 5-HT$_6$R also induces neurite outgrowth through Cdk5 activation, a process leading to the phosphorylation of a serine residue in the C-terminal tail of the receptor (Ser^{350}) and the activation of Cdc42 and its downstream signaling pathway (Duhr et al., 2014). Once neurite outgrowth has been initiated, the receptor no more interacts with Cdk5 and associates with another protein partner, G Protein-Regulated Inducer of Neurite Growth 1 (GPRIN1). This association enhances receptor-mediated cAMP production, which in turn activates PKA and promotes the branching of neurites(Pujol et al., 2020). Interestingly, neuronal migration and

* Corresponding author at: Institut de Génomique Fonctionnelle, 141, rue de la Cardonille, F-34094 Montpellier Cedex 5, France.
E-mail address: severine.chaumont-dubel@igf.cnrs.fr (S. Chaumont-Dubel).
[1] These authors contributed equally to the study.

https://doi.org/10.1016/j.nbd.2022.105949
Received 17 October 2022; Received in revised form 25 November 2022; Accepted 5 December 2022
Available online 7 December 2022

neurite outgrowth under the control of 5-HT$_6$R are mediated by constitutive (5-HT-independent) receptor activation.

The 5-HT$_6$R is also able to engage the mechanistic Target Of Rapamycin (mTOR) pathway. Aberrant 5-HT$_6$R-operated mTOR signaling has been involved in cognitive deficits observed in several pathological conditions caused by neurodevelopmental alterations, such as rodent models of schizophrenia, Neurofibromatosis type 1 and cannabis abuse during adolescence (Berthoux et al., 2020; Deraredj Nadim et al., 2016; Doucet et al., 2021; Meffre et al., 2012). Although the mTOR pathway has been identified as a key regulator of neuro-developmental processes, the role of mTOR signaling in neuronal migration and neurite outgrowth dependent on 5-HT$_6$R remains to be established. Likewise, the link between perturbed cognition induced by aberrant activation of the 5-HT$_6$R-mTOR pathway and neurodevelopmental processes controlled by the 5-HT$_6$R needs to be elucidated.

Despite the growing interest in this receptor, little is known about its precise spatio-temporal (sub)cellular localization pattern during brain development and in adulthood. Several studies using RT-PCR, *in situ* hybridization, radioactive ligand binding or BAC transgenic mice have sought to describe its expression and location in the human and rodent central nervous systems. They showed that the 5-HT$_6$R is almost exclusively expressed in the central nervous system, especially in areas associated with higher cognitive functions, such as the striatum, the cortex and the hippocampus (Gerard et al., 1996; Gerard et al., 1997; Helboe et al., 2015; Hirst et al., 2003; Kohen et al., 1996; Monsma Jr. et al., 1993; Ruat et al., 1993; Yoshioka et al., 1998). However, some of these studies lead to contradictory results, depending on whether protein or mRNA expression were examined. Furthermore, they did not provide any information on the subcellular localization of the receptor.

To address this issue, we developed a new knock-in mouse line expressing 5-HT$_6$R fused to green fluorescent protein (GFP) on its C-terminal extremity (Htr6-GFP KI mice), as well as a mouse embryonic stem cell line expressing the 5-HT$_6$R tagged with GFP. Using a combination of immunofluorescence and confocal microscopy, we provide an extensive description of the expression pattern of the 5-HT$_6$R in the mouse central nervous system at embryonic, neonatal and adult stages, and characterized the cell types expressing the receptor. Analysis of receptor subcellular localization also showed a transient relocation of the receptor from primary cilia to the somato-dendritic compartment in certain neuronal subpopulations at the neonatal stage (from P1 to P10). Hence, this study provides the first extensive characterization of the spatio-temporal expression of native 5-HT$_6$R that might help understanding its modulation of brain circuitry shaping and cognitive functions.

2. Results

2.1. Expression of the 5-HT$_6$R in adult mouse brain

In adult mouse brain, the 5-HT$_6$R was detected in the cortex, the olfactory bulbs, the CA1, CA2 and CA3 areas of the hippocampus, the dorsal striatum, the nucleus accumbens, the hypothalamus and the septum (Fig. 1). In agreement with its role in neuropathic pains of different etiologies (Martin et al., 2020), it was also found in the dorsal and ventral horns of the spinal cord (Fig. 1). We did not detect 5-HT$_6$R expression in any of the thalamic nuclei, as exemplified here for the medio-dorsal nucleus, nor in the cerebellum (Supplementary Table 1 and Fig. 1), corroborating *in situ* hybridization studies (Helboe et al., 2015). Collectively, these findings indicate that the receptor is expressed in a wide range of brain structures, including those involved in higher cognitive functions, such as the cortex, hippocampus and striatum, where the cellular and subcellular expression patterns were explored in further experiments.

The 5-HT$_6$R immunoreactivity was mostly detected in primary cilia in adult brain, as assessed by its colocalization with Adenylate Cyclase 3 (AC3) (Fig. 2). Interestingly, the majority of AC3-positive cilia co-express 5-HT$_6$R in the three brain regions (Fig. 2, top histogram). Nevertheless, 5-HT$_6$R immunostaining was also detected in structures that morphologically resemble primary cilia but do not show AC3 immunoreactivity. Whereas AC3 is a marker of neuronal cilia in adult brain, Arl13b is rather considered as a marker of astrocytic cilia (Sipos et al., 2018; Sterpka and Chen, 2018; Sterpka et al., 2020).

To confirm the cellular specificity of these ciliary markers in our model, we performed co-immunostaining of AC3 with the neuronal marker NeuN, and of Arl13b with either GFAP (hippocampus) or S100ß (cortex and striatum) (Jurga et al., 2021). As shown on Fig. S1, in the hippocampus, the cortex and the striatum, AC3-positive cilia were exclusively found on NeuN-positive cells, whereas Arl13b-positive cilia were detected on astrocytes. To determine if 5-HT$_6$R-positive cilia lacking AC3 are positive for Arl13b, we realized co-immunostaining of 5-HT$_6$R with both cilia markers and found that 5-HT$_6$R immunostaining was co-localized with either AC3 or Arl13b labeling (Fig. 2). This indicates that the receptor is located in the primary cilium of both neurons and astrocytes in the adult brain.

Taking advantage of the specificity of Arl13b for astrocytic cilia and AC3 for neuronal cilia, we quantified the proportion of neuronal and astrocytic cilia expressing the 5-HT$_6$R. Almost all AC3-positive cilia express the 5-HT$_6$R in the hippocampus and striatum (98.02 ± 1.37% and 98.70 ± 0.99% respectively), whereas the percentage of AC3-5HT$_6$R co-labeled cilia is 76.49 ± 5.41% in the cortex (Fig. 2, top histogram). About half of astrocytic Arl13b-positive cilia express the 5HT$_6$R in the hippocampus (55.35 ± 9.75%) and the striatum (52.21 ± 16.14%). This proportion is slightly higher in the cortex (68.32 ± 4.71%) (Fig. 2, middle histogram). Finally, in all three structures, most of the 5-HT$_6$R-positive cilia are found on neurons (94.68 ± 0.52% in the hippocampus, 93.69 ± 2.96% in the striatum, and 81.84 ± 4.08% in the cortex), with the remaining 5-HT$_6$R-positive cilia being associated with astrocytes (Fig. 2, bottom histogram).

We then sought to determine the neuronal populations expressing the 5-HT$_6$R. To assess the presence of the receptor on interneurons, we co-labeled GABA and 5-HT$_6$R in the cortex and the hippocampus (Fig. 3A). We show that only 9.04 ± 3.98% of GABAergic interneurons bear 5-HT$_6$R-positive cilia in the cortex (Fig. 3A, left histogram). Overall, <1% of 5-HT$_6$R-positive cilia (0.89 ± 0.33%) were found on GABAergic interneurons (Fig. 3A, right histogram). Likewise, only a minority of GABAergic interneurons express 5-HT$_6$R-positive cilia in the hippocampus (Fig. 3A). We then labeled projection neurons (Fig. 3B).

We used DARPP-32 and Wolframin (WFS1) to label medium-sized spiny neurons (MSN) in the striatum and pyramidal neurons in the hippocampus, respectively. In the striatum, most 5-HT$_6$R-positive cilia are associated to MSNs (Fig. 3B). In the hippocampus, the receptor is mainly found on WFS1-positive pyramidal neurons (Fig. 3B). Taken together, these data suggest that most of 5-HT$_6$Rs are localized on projection neurons rather than interneurons in the different brain regions we examined.

2.2. The 5-HT$_6$R locates in somatodendritic compartment of certain neuronal populations at the neonatal stage

To determine if the subcellular location of the receptor varies during development, we first examined its expression pattern in coronal brain slices from Htr6-GFP KI mice, at E13.5 and E17.5 (Fig. S2). Corroborating previous observations (Jacobshagen et al., 2014), we detected 5-HT$_6$R expression as early as E13.5 in the cortex, the ventricular zone (VZ), and the striatum (Fig. S2A). The receptor was also found to a lesser extent in the subventricular zone (SVZ) (Fig. S2A). Higher density of receptor expression was found at E17.5 in the same regions (Fig. S2B). At both developmental stages, 5-HT$_6$R immunolabeling appears as small puncta reminiscent of the morphology of the protocilium (Arellano et al., 2012). While Arl13b consistently labels developing primary cilia in the embryonic brain, the expression level of AC3 is low in protocilium (Paridaen et al., 2013). Consistent with these findings, 5-HT$_6$R

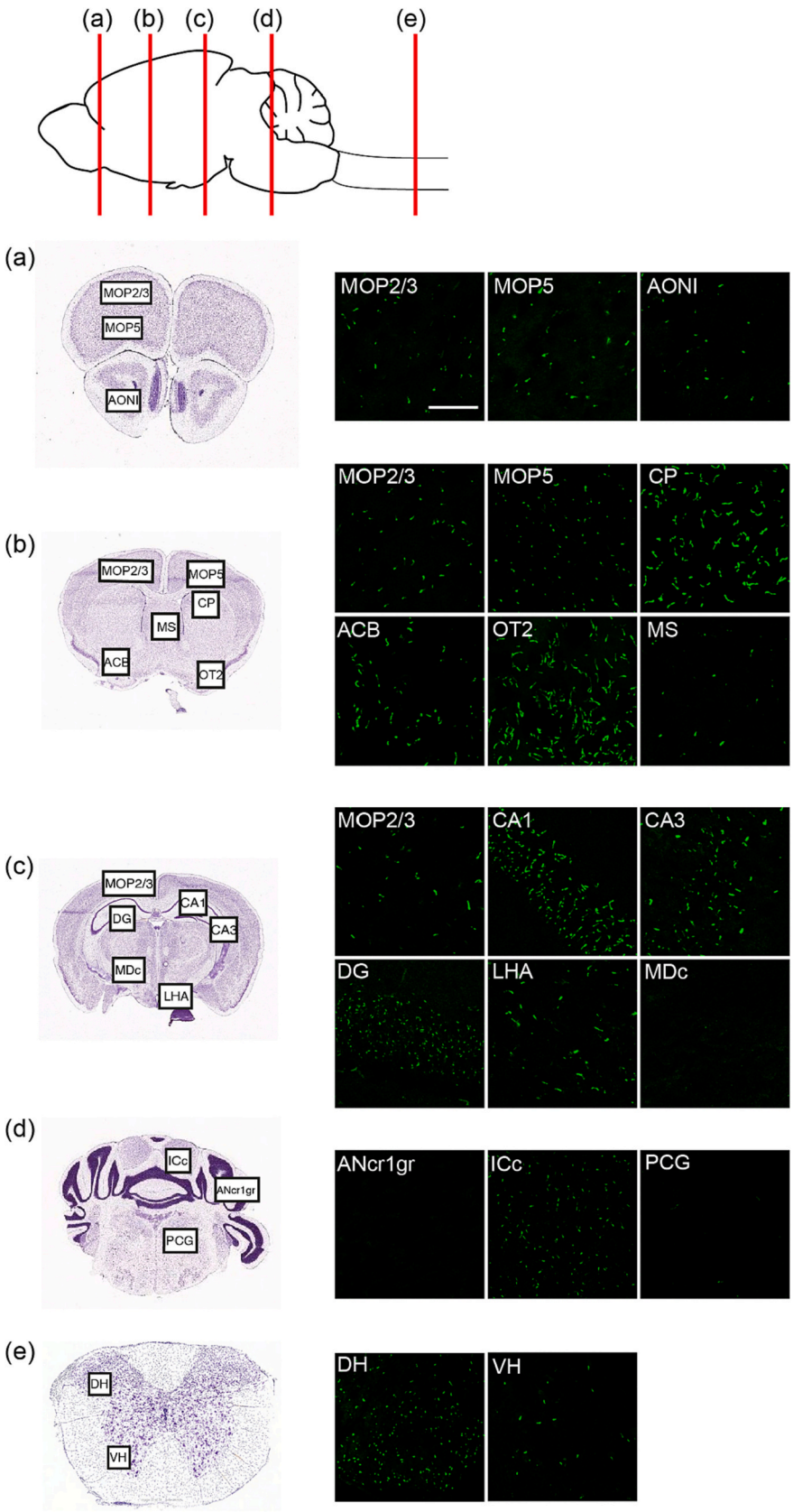

Fig. 1. Regional distribution of the 5-HT$_6$R in mouse adult brain.

Coronal brain and spinal cord sections (50 μm) were obtained at five different levels from Htr6-GFP KI adult mice, as illustrated. (a)-(e) The left panel shows images from the Mouse Brain Atlas (https://mouse.brain-map.org) illustrating where the sections depicted on the right were obtained. The right panel shows confocal images of 5-HT$_6$R immunolabeling performed using an anti-GFP antibody. Abbreviations were taken from the Mouse Brain Atlas: MOP2/3, primary motor area layer 2/3; MOP5, primary motor area layer 5; AONI, anterior olfactory nucleus lateral part; CP; caudate putamen; Acb, nucleus accumbens; OT2, olfactory tubercles pyramidal layer; MS, Medial septal nucleus; CA1 and CA3, field CA1 and CA3 stratum radiatum; DG, dentate gyrus molecular layer; LHA, Lateral hypothalamic area; MDc, Mediodorsal nucleus of the thalamus central part; ANcr1gr, crus1 granular layer; ICc, inferior colliculus central nucleus, PCG, pontine central gray; VH, ventral horn of spinal cord; DH, dorsal horn of spinal cord. Scale bar: 10 μm.

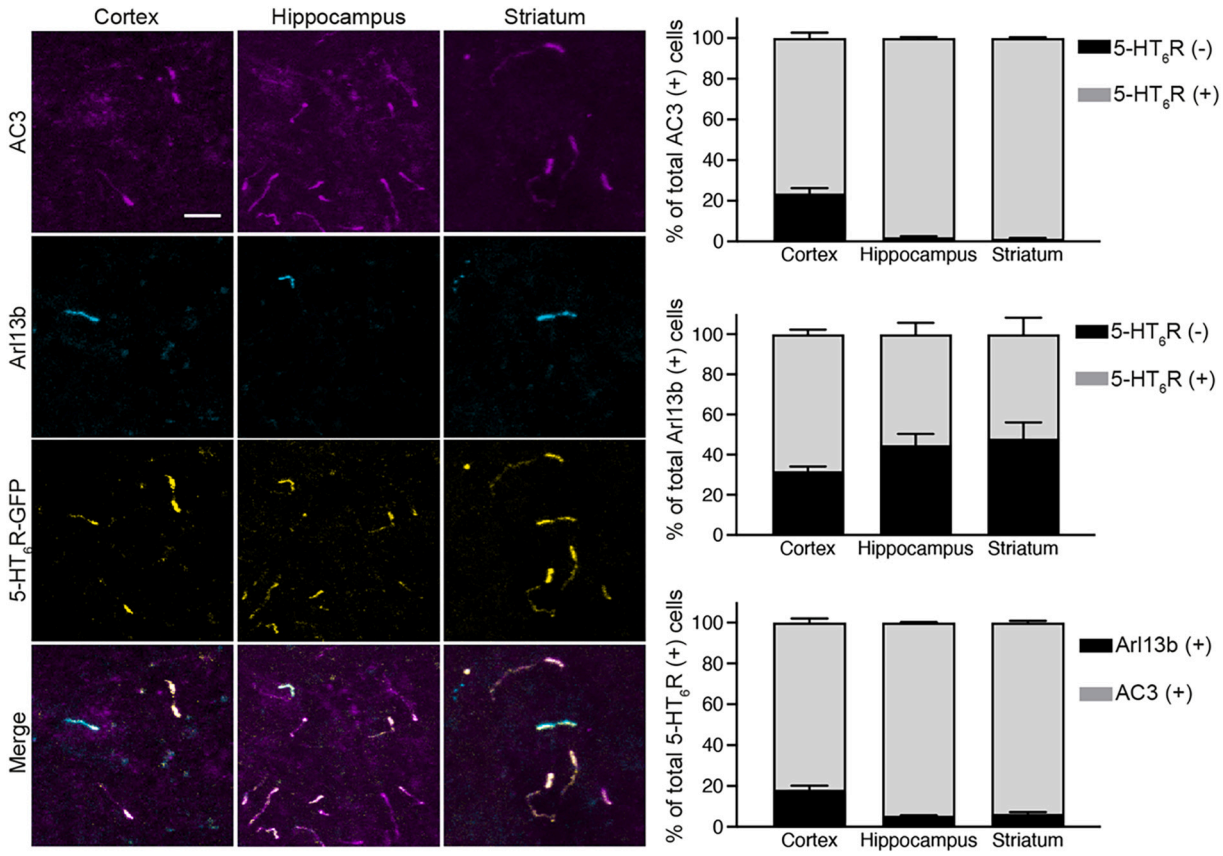

Fig. 2. Localization of the 5-HT$_6$R in primary cilia in neurons and astrocytes.
Confocal images of AC3 (magenta), Arl13b (cyan) and 5-HT$_6$R-GFP (yellow) immunolabeling in 50-µm coronal brain sections from adult Htr6-GFP mouse cortex (layer V), hippocampus (CA1) and dorsal striatum (scale bar 10 µm). The histograms on the right show quantifications in the three structures. The top histogram shows the percentage of cells expressing AC3 and 5-HT$_6$R (gray) or AC3 alone (black). The number of quantified cilia is $n = 813$ from four animals in the cortex, $n = 580$ cilia from three animals in the hippocampus and $n = 3110$ cilia from ten animals in the striatum. The histogram in the middle represents the percentage of cells expressing Arl13b and 5-HT$_6$R (gray) or Arl13b alone (black). The number of quantified cilia is $n = 197$ from four animals in the cortex, n = 58 cilia from 3 animals in the hippocampus and $n = 451$ cilia from 10 animals in the striatum. The bottom histogram shows the percentage of 5-HT$_6$R-positive cells expressing either AC3 (gray) or Arl13b (black). The number of quantified cilia is $n = 765$ from four animals in the cortex, $n = 600$ cilia from three animals in the hippocampus and $n = 3273$ cilia from 10 animals in the striatum. Data are means ± SEM.

immunostaining was mainly found in structures expressing Arl13b, indicating its ciliary localization in the developing brain (Fig. S3). 5-HT$_6$R and Arl13b were only partially co-localized with AC3, particularly in the VZ (Fig. S2).

We previously demonstrated that the 5-HT$_6$R is detected both in the primary cilium and the soma of neurons in 5-HT$_6$-GFP KI mice at the neonatal stage, when dendrite complexification occurs (Pujol et al., 2020). Furthermore, we found that 5-HT$_6$R specifically associates with its protein partner GPRIN1 in the soma plasma membrane, while no colocalization between 5-HT$_6$R and GPRIN1 was detected in the primary cilium (Pujol et al., 2020). Fig. 4A shows the expression of the receptor from post-natal day 1 (P1) to post-natal day 30 (P30) in the striatum.

Corroborating our previous observations, the receptor is located in both the primary cilium (arrowheads) and the soma (arrows) of neurons in the striatum from Htr6-GFP KI mice at P1 (Fig. 4A). At P3 and P7, most of the 5-HT$_6$R immunostaining was found at the soma membrane, whereas at P10 and afterward, the receptor was detected in primary cilia (Fig. 4A). We wondered if the transient relocation of the receptor in soma occurs everywhere in the brain or if it is restricted to certain brain areas. As shown on Fig. S3A, the receptor is mainly located in the soma of neurons in most brain regions at P5, including deep layers of the cortex (DCLs), septum, and striatum. However, the receptor remains localized in the primary cilium in the outer layers of the cortex (OCL, Fig. S3A, area 2). We quantified the percentage of somatic and ciliary receptors in the striatum, DCL and OCL at P7 and P30 (Fig. S3B). At P7, the receptor was at the soma membrane in 56.80 ± 9.20% of striatal cells and 62.08 ± 12.71% of DCL cells. In OCL, no labeling was detected in the soma. The percentage of 5-HT$_6$R-positive cilia represented 22.80 ± 5.64% of striatal cells, 8.20 ± 4.01% DCL cells, and 14.73 ± 2.59% of OCL cells (Fig. S3B top histogram). At P30, no somatic labeling was detected in any of the three structures. The percentage of cells showing ciliary localization of the receptor was 74.08 ± 7.63% in the striatum, 39.27 ± 2.36% in DCL cells and 37.89 ± 5.16% in OCL cells (Fig. S3B bottom histogram).

As observed in the adult brain, co-immunostaining of GABA and 5-HT$_6$R in the cortex at P5 showed that very few interneurons express the receptor (blue arrows, Fig. S4, top panels). Most receptor labeling appears on GABA-negative cells (white arrows, Fig. S4, top panels). Co-labeling of DARPP32 and 5-HT$_6$R in the striatum at P5 indicated that most of the cells expressing the 5-HT$_6$R at the soma membrane are MSNs (white arrows, Fig. S4, bottom panels). Interestingly, we also detected a few 5-HT$_6$R-positive structures resembling primary cilium (arrowheads, Fig. S4, bottom panels), but none of them were found on DARPP32-positive neurons, suggesting that they could be astrocytes. Collectively, these observations indicate that the receptor is expressed in the same populations of neurons at P5 and in adulthood.

In line with previous findings indicating that 5-HT$_6$R overexpression results in its expression outside of the cilia (Brodsky et al., 2017), we examined whether receptor relocation to the soma membrane at perinatal stages might be caused by an increase in its expression. qRT-PCR

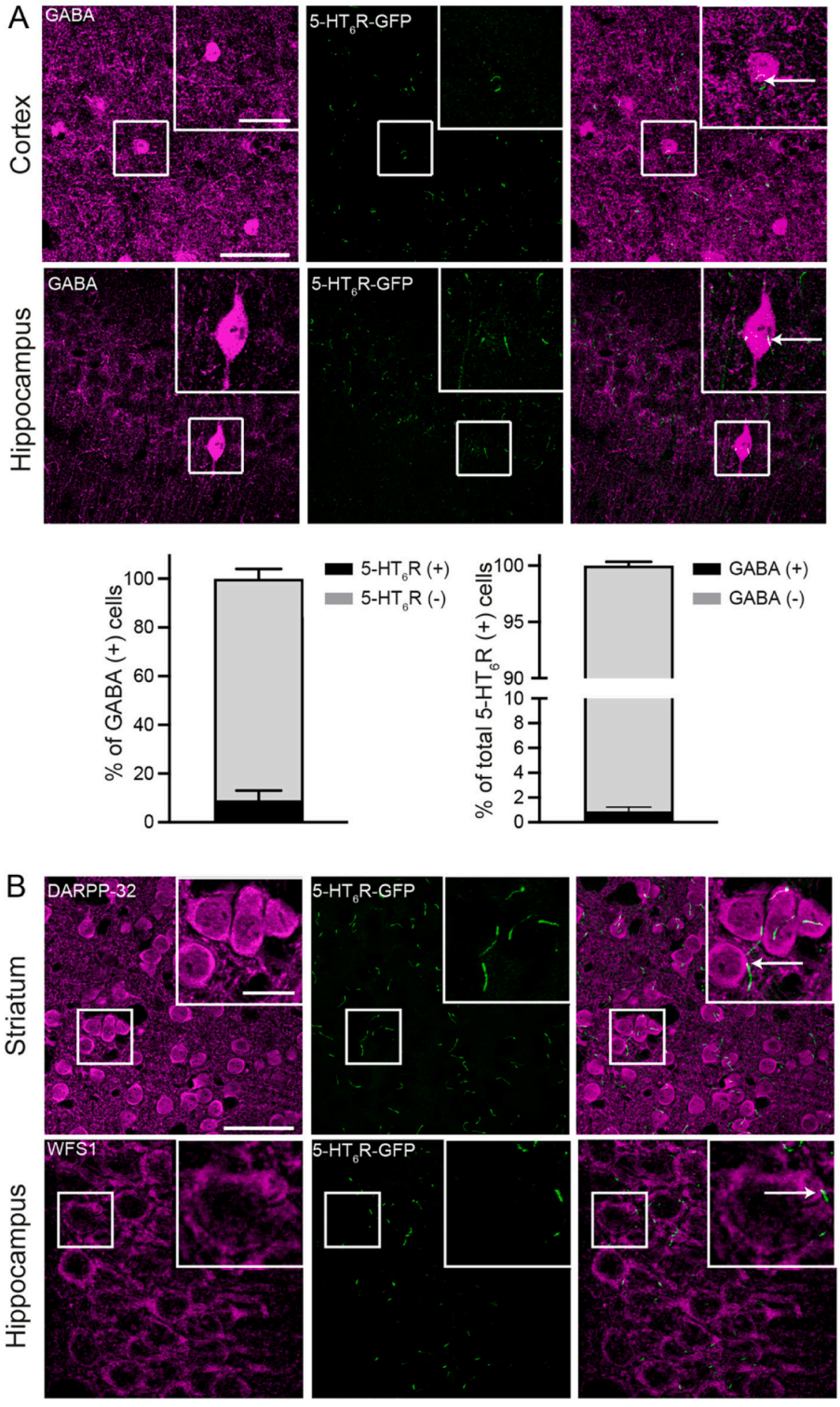

Fig. 3. 5-HT_6R expression in projection neurons and GABAergic interneurons.
(A) Confocal images of 5-HT_6R-GFP (green) and GABA (magenta) co-immunostaining in cortex and hippocampus from adult Htr6-GFP mice (scale bar 50 μm). Regions delineated with a white square are shown enlarged at the top right of the picture (scale bar 20 μm). White arrows show 5-HT_6R-positive cilia associated with interneurons. The left histogram represents the percentage of GABA-positive cells with 5-HT_6R-positive cilia (n = 115 neurons from 6 animals counted). The right histogram shows the percentage of cells positively stained with the GABA antibody and displaying 5-HT_6R-positive cilia (n = 726 neurons from 6 animals counted). Data are means ± SEM. (B) Confocal images of 5-HT_6R-GFP (green) and either DARPP32 or wolframin1 (magenta) co-immunostaining in the striatum and hippocampus from adult Htr6-GFP mice (scale bar 50 μm). Regions delineated with a white square are shown enlarged at the top right of the picture (scale bar 20 μm). White arrows show 5-HT_6R-positive cilia associated with MSNs (DARPP32-positive) in the striatum and projection excitatory neurons (WFS1-positive) in the hippocampus. The illustrated images are representative of six independent experiments performed on slices from different animals.

analysis of 5-HT_6R mRNA extracted from the striatum at E13.5, E17.5, P1, P7, P10 and P30 showed that 5-HT_6R expression is strongly enhanced between E13.5 and E17.5 and keeps increasing until birth (Fig. 4B). Thereafter, the expression of the receptor slightly increases up to the adult stage (Fig. 4B). This indicates that the 5-HT_6R expression level is not correlated with its subcellular localization during brain development and that the transient relocation of the receptor to the soma membrane at the neonatal stage is not due to its overexpression.

As the primary cilium is a dynamic structure that can be remodeled during development, we also checked if cilia are present at the neonatal stage in brain regions where the receptor is mainly expressed at the soma membrane, such as the inner layers of the cortex (Fig. S3). We estimated the number of cells exhibiting either AC3- or Arl13b-positive cilia in the striatum at P7 and at P30 (Fig. 4C). At P7, only 15.75 ± 1.37% of the cells possess an AC3-positive cilium, whereas at P30, this percentage is more than three times higher (53.15 ± 2.80%) (Fig. 4C). Interestingly

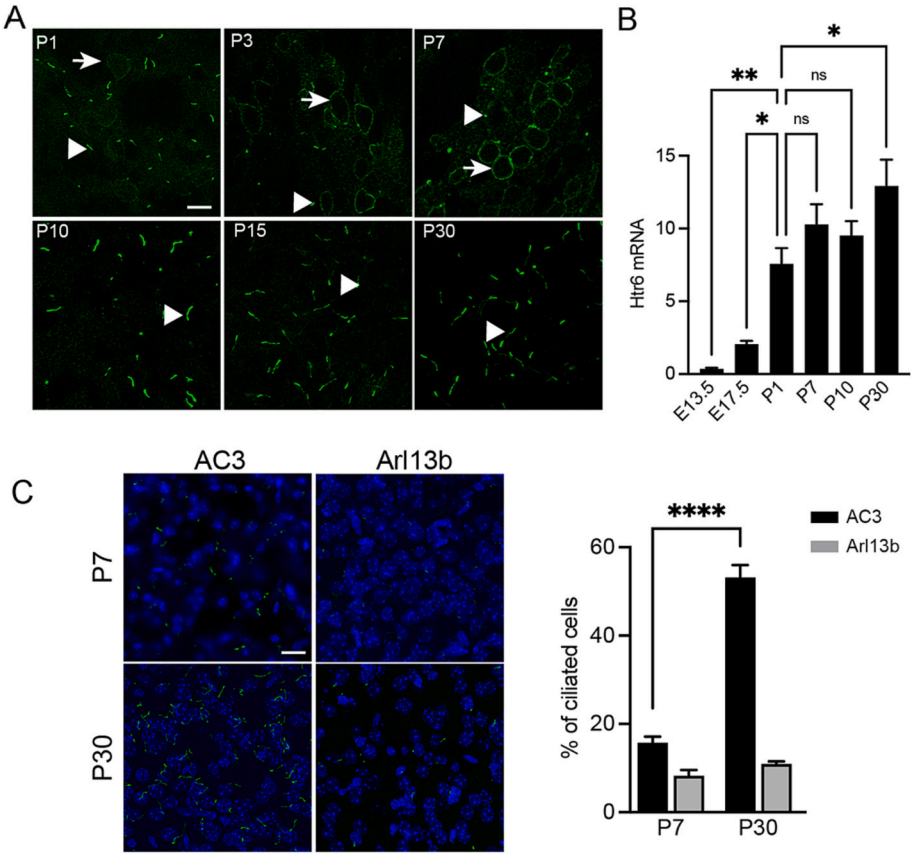

Fig. 4. Dynamic changes of 5-HT$_6$R subcellular localization at the neonatal stage.
(A) Confocal images of 5-HT$_6$R-GFP immunostaining (green) using an anti-GFP antibody in the striatum of mice from perinatal to adult stages (P1 to P30) (scale bar 10 μm). Arrows show the somatic expression of the receptor, while arrowheads point at the ciliary receptor. (B) q-PCR analysis of 5-HT$_6$R mRNA level in striatum at E13.5, E17.5, P1, P7, P10 and P30. Control q-PCR was performed in the cerebellum, a structure that does not express the receptor. * $p <$ 0.05 and ** $p < 0.001$, one-way ANOVA followed by Dunnett's multiple comparison test. (C) Confocal images showing a representative field in the striatum at P7 and P30. Nuclei are stained with DAPI (Blue), and primary cilia are labeled with either AC3 or Arl13b as indicated above the images (green). The histogram shows the quantification of the number of ciliated cells. Quantification was done on slices from three or four animals, and the total number of cells assessed was at P7 328 for AC3 and 640 for Arl13b, and at P30 847 for AC3 and 478 for Arl13b. **** $p <$ 0.0001, all groups were compared using one-way ANOVA followed by Tukey's multiple comparison test.

the percentage of Arl13b-positive cilia is lower and does not change significantly between P7 and P30 (8.28 ± 1.31% and 10.92 ± 0.58%, respectively) (Fig. 4C).

To further examine the dependency of the 5-HT$_6$R subcellular localization on the presence of the primary cilium at different developmental stages, we took advantage of a neurodevelopment model based on embryonic stem cells (ESCs) differentiation into neurons (Gaspard et al., 2009). It was previously reported that pluripotent ESCs are poorly ciliated and that the proportion of ciliated cells increases as cells exit from pluripotency (Kiprilov et al., 2008). We generated a mouse transgenic ESC line that expresses the 5-HT$_6$R tagged with GFP under the control of a doxycycline-inducible promoter. We used a similar cell line expressing cytosolic GFP as control and induced the expression of the cytosolic GFP or of the receptor either at the ES stage or four days after starting the differentiation of the cells (J4) (Fig. 5).

Confirming previous findings (Kiprilov et al., 2008), we observed that very few pluripotent (undifferentiated) ESCs possess a primary cilium (labeled with an anti-Arl13b antibody) and that the proportion of cilia-positive cells strongly increases upon differentiation (Fig. 5 ES *vs.* J4 panel). In undifferentiated cells, the 5-HT$_6$R is mainly found in the soma (white arrows), and in a few cilia (arrowheads). In contrast, in differentiated/ciliated cells, the receptor localizes to the cilium (Fig. 5). Note that cytosolic GFP never exhibits a ciliary localization. This is highly reminiscent of what is seen *in vivo*, where the receptor localizes to the cilium when it is present after neuronal differentiation and is found in the soma in cilia-less, and probably immature neurons.

2.3. The 5-HT$_6$ receptor influences primary cilia morphology

Several lines of evidence suggest that 5-HT$_6$Rs regulate primary cilia morphology: while overexpressing 5-HT$_6$Rs in striatal and hippocampal neurons increases cilia length, 5-HT$_6$R blockade induces a reduction of cilia length (Brodsky et al., 2017; Hu et al., 2017; Lesiak et al., 2018). However, these observations were made in primary cultured neurons, using Arl13b as a cilia marker. No data showing the influence of the receptor on cilia morphology *in vivo* is available. To explore whether 5-HT$_6$R likewise affects the morphology of cilia in adult mouse brain, we compared the length of primary cilia in brain slices from wild-type (WT) and Htr$_6$-KO mice. As shown on Fig. 6, primary cilia are significantly shorter in Htr$_6$-KO animals compared to WT animals. The largest effect was seen in the striatum, whereas hippocampal cilia were the least affected by the genetic deletion of the receptor (Fig. 6).

3. Discussion

The 5-HT$_6$R is one of the most recently discovered serotonin receptors and has emerged as a promising therapeutic target to prevent cognitive symptoms associated with several neuropsychiatric disorders, such as schizophrenia and autism spectrum disorders. Several studies have shown that 5-HT$_6$R blockade improves cognition in various rodent models of cognitive impairment (Berthoux et al., 2020; Codony et al., 2011; de Bruin et al., 2016; Doucet et al., 2021; Grychowska et al., 2016; Hirst et al., 2006; Meffre et al., 2012). Pro-cognitive effects of 5-HT$_6$R antagonists have also been demonstrated in humans, and several clinical trials have been initiated to evaluate their efficacy to counter the cognitive decline in several neurodegenerative or psychiatric diseases (Ferrero et al., 2017; Li et al., 2021; Morozova et al., 2017; Wilkinson et al., 2014). The 5-HT$_6$R also strongly influences key neurodevelopmental processes, such as neuron migration (Jacobshagen et al., 2014; Riccio et al., 2009) and neurite growth (Duhr et al., 2014; Guadiana et al., 2013; Lesiak et al., 2018; Pujol et al., 2020; Rahman et al., 2017) However, the mechanisms underlying the role of 5-HT$_6$R in neurodevelopment and cognition are still not entirely known. Important advances have been made with the discovery of alternative signal transduction mechanisms engaged by the receptor in addition to the canonical Gs-adenylyl cyclase pathway. For instance, a non-

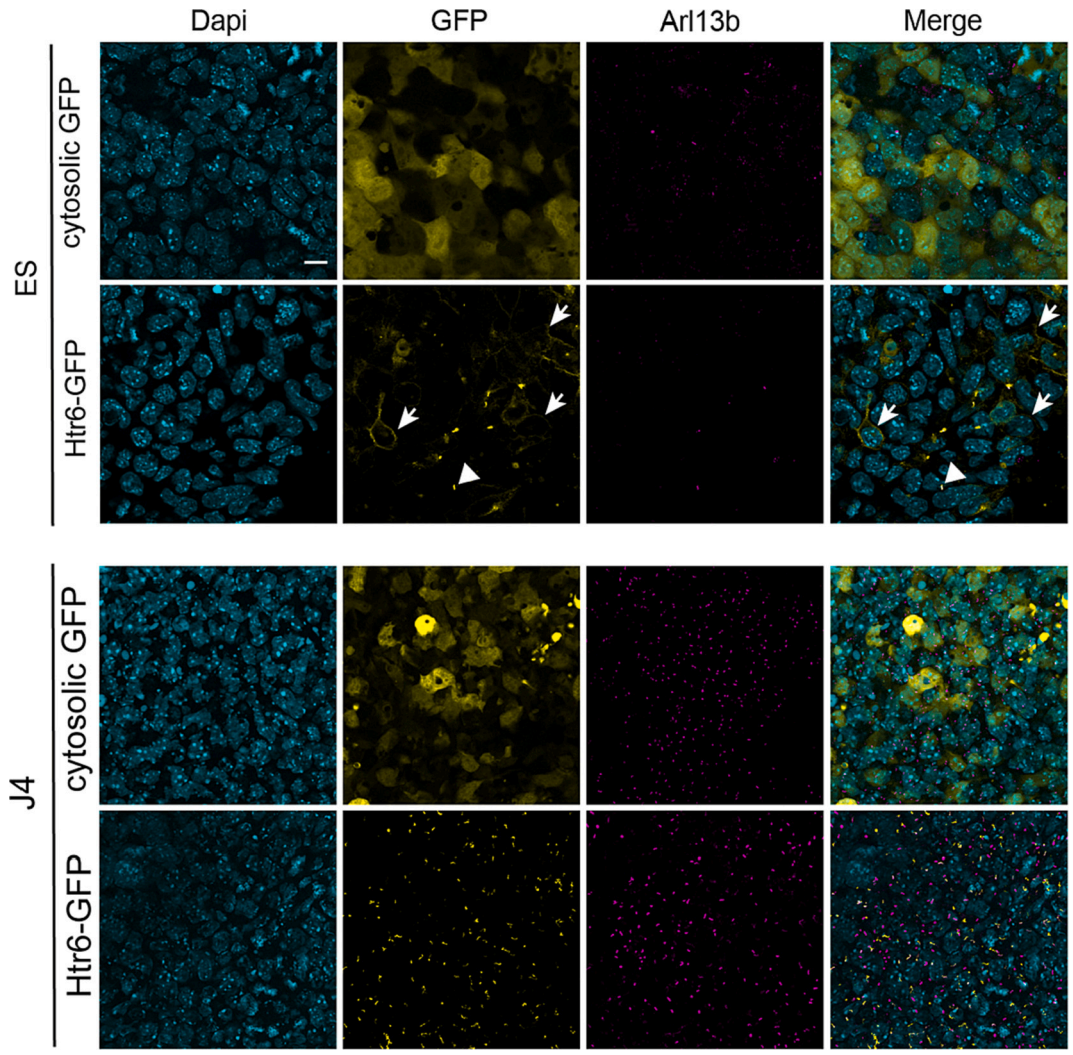

Fig. 5. The 5-HT$_6$R is predominantly expressed in the soma of ES cells, but in the primary cilium of differentiated cells.
Confocal images of the expression of GFP (yellow) and Arl13b (magenta) in mouse A2Lox.cre stem cells expressing either cytosolic GFP or Htr6-GFP under the control of a doxycycline-inducible promoter. Dapi was used to stain all nuclei (cyan). Cells were treated with 1 μg/ml of doxycycline for 24 h before fixation. The top panel shows undifferentiated cells, whereas the bottom panel shows cells differentiated for 4 days prior to doxycycline induction. Arrows point to somatic 5-HT$_6$R whereas arrowheads point to the ciliary receptor. Scale bar: 10 μm.

physiological activation of the mTOR pathway induced by 5-HT$_6$R was found to mediate cognitive deficits in developmental models of schizophrenia (Meffre et al., 2012), cannabis abuse during adolescence (Berthoux et al., 2020) and Neurofibromatosis type1 (Doucet et al., 2021). Neuron migration and initiation of neurite outgrowth under the control of the 5-HT$_6$R depend on activation of Cdk5 signaling (Chaumont-Dubel et al., 2020; Duhr et al., 2014; Guadiana et al., 2013; Lesiak et al., 2018; Pujol et al., 2020; Rahman et al., 2017). However, an important limitation in understanding receptor functions in developing and adult brains is the uncertain receptor localization at the cellular and subcellular levels. Discrepancies between studies might be due to the different species examined (human, rat, and mouse) or to the use of different experimental approaches (*in situ* hybridization, immunohistochemistry, or radioligand binding). For instance, using double *in situ* hybridization in the rat, Helboe et al. did not detect 5-HT$_6$R mRNA in the cerebellum (Helboe et al., 2015), whereas Gerard et al. found a substantial expression of the receptor protein in this region by immunohistochemistry (Gerard et al., 1997). This underlines the need to test commercially available antibodies on knock-out models to ascertain their specificity.

To overcome these issues and get a precise picture of the expression pattern of the 5-HT$_6$R protein in mouse brain, not only at the regional but also at the cellular and subcellular levels, we used a KI mouse line that endogenously expresses 5-HT$_6$R fused to GFP. Consistent with the key role of 5-HT$_6$R in cognition, we observed a robust expression of the receptor in regions involved in higher cognitive functions, such as the nucleus accumbens, cerebral cortex or hippocampus, where it is present in CA1, CA2 and CA3 regions as well as dentate gyrus. In line with the ability of 5-HT$_6$R ligands to reduce food intake and obesity, the receptor is also strongly expressed in the hypothalamus, a brain region involved in the regulation of food intake and energy expenditure. Finally, consistent with a previous study showing a role of spinal 5-HT$_6$R constitutive activity in the maintenance of neuropathic pains of different etiologies, the receptor was also detected in the spinal cord (Martin et al., 2020), whereas it was absent in the cerebellum. Overall, these findings are consistent with the previously described 5-HT$_6$R mRNA expression pattern in rat neurons (Helboe et al., 2015; Monsma Jr. et al., 1993; Ruat et al., 1993), thus validating our Htr6-GFP KI model and further supporting the relevance of mouse models to study the receptor.

The neuronal subtypes expressing the receptor also remain controversial. Studies have shown that pharmacological inhibition of the receptor in rats enhances cholinergic and excitatory transmissions in cortex and hippocampus (Codony et al., 2011). This led to the hypothesis that the receptor could be predominantly expressed by inhibitory interneurons, where its blockade would relieve GABAergic inhibition,

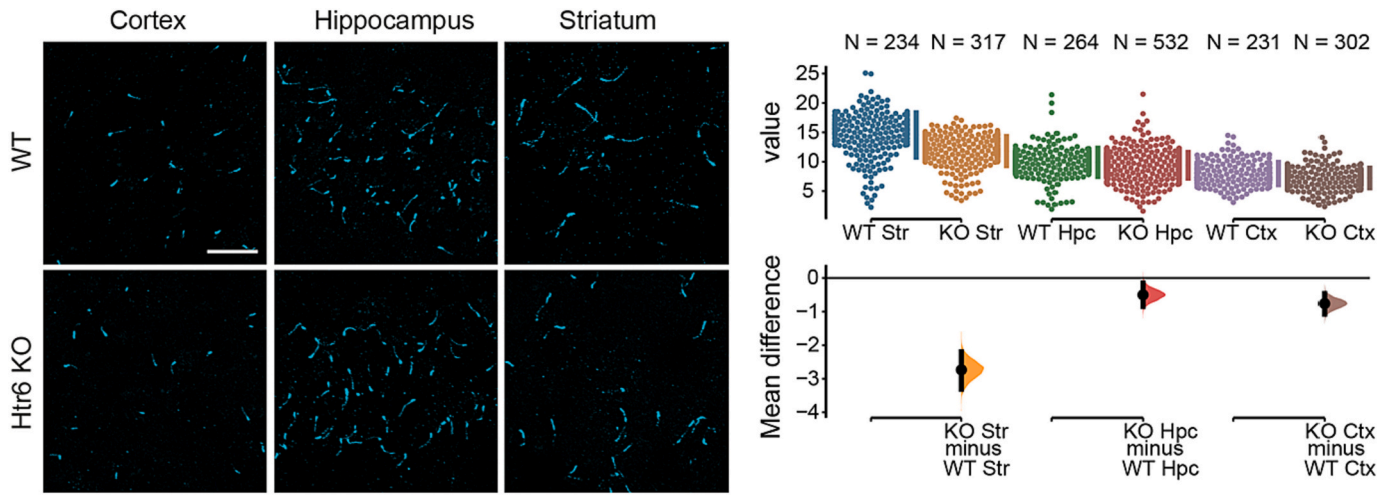

Fig. 6. Cilia length regulation by 5-HT$_6$R expression.
Confocal images showing representative fields from cortex, hippocampus or striatum sections of Wild-Type and Htr6-KO adult mice immunolabeled with the AC3 antibody (scale bar 20 μm). The Cumming estimation plots show the mean differences of cilia length in KO *vs.* WT mice in the three brain regions examined. It represents data obtained in three independent experiments performed on different animals. The raw data are plotted on the upper axes; each mean difference is plotted on the lower axes as a bootstrap sampling distribution. Mean differences are depicted as dots; 99% confidence intervals are indicated by the ends of the vertical error bars. The unpaired mean difference between WT and KO striatum is −2.73 [99.0%CI -3.45, −2.01]. The *P* value of the two-sided permutation *t*-test is 0.0. The unpaired mean difference between WT KO hippocampus is −0.501 [99.0%CI -0.968, −0.0389]. The *P* value of the two-sided permutation t-test is 0.0026. The unpaired mean difference between WT and KO cortex is −0.761 [99.0%CI -1.18, −0.358]. The *P* value of the two-sided permutation t-test is 0.0. The effect sizes and CIs are reported above as: *effect size* [*CI width lower bound;upper bound*] (Ho et al., 2019) . Scale bar: 10 μm.

causing an increased release of other neurotransmitters like acetylcholine and glutamate to promote cognitive processes. This hypothesis was invalidated by the study of Helboe et al. which showed that the receptor is predominantly expressed in projection neurons, while 5-HT$_6$R mRNA was only detected in a little proportion of GABAergic interneurons (Helboe et al., 2015). Corroborating these observations, we show that GABAergic interneurons represent <1% of the cells expressing the receptor in mouse cortex. Though quantification in hippocampus is challenging because of the density of cell bodies, the receptor is almost exclusively present in the projection neuron layers. How blockade of 5-HT$_6$Rs expressed in primary excitatory neurons would promote cholinergic and glutamatergic transmission certainly warrants further exploration. Furthermore, in the striatum, we found a clear association of 5-HT$_6$R-positive primary cilia and MSNs. The 5-HT$_6$R is coupled to G$_S$, thus increasing cAMP production and neuronal excitability. One possibility is that the cognition-enhancing effects of 5-HT$_6$R antagonists involve the inhibition of receptors expressed in MSNs and complex neuronal circuits comprising MSNs.

In the embryonic brain, the nature of neurons expressing the receptor may be different. We show that at E17.5, the receptor is predominantly expressed in Arl13b positive proto-cilia, which are found on immature cortical neurons as well as migrating interneurons, (Higginbotham et al., 2012).This is consistent with the observation of Riccio *et al*, showing that the 5-HT$_6$R is involved in the migration of cortical interneurons (Riccio et al., 2009). Once neurons have reached their final destination, the cilium disappears and is then rebuilt during post-migratory ciliogenesis (Sarkisian and Guadiana, 2015). It is likely that the cilia of post-migratory interneurons do not express the same proteins as the primary cilia of migratory interneurons, which would account for the lack of expression of the 5-HT$_6$R in mature cortical interneurons.

One important discrepancy between the present work and the study conducted by Helboe et al. is the presence of the receptor in astrocytes. Helboe et al. concluded that the 5-HT$_6$ receptor is exclusively expressed in neurons in the rat, as 5-HT$_6$R mRNA was absent in any GFAP expressing astrocytes (Helboe et al., 2015). However, some studies have shown 5-HT$_6$R expression in rat cultured astrocytes (Hirst et al., 1998; Hirst et al., 1997) and in an astrocytic cell line (Vanda et al., 2018). Corroborating these observations, we show that a large proportion of astrocytes express the receptor in their primary cilia in the cortex, hippocampus, and striatum. The role of 5-HT$_6$R expressed in astrocytes remains largely unknown, but studies performed on the C8-D1A astrocyte cell line suggest that the receptor constitutive activity might be involved in 6-OHDA-induced astrocyte death (Vanda et al., 2018).

The subcellular localization of the 5-HT$_6$R also remains debated. Initial immunohistochemical studies showed that it is present on dendrites and dendritic spines (Gerard et al., 1997) but also on cilia-like structures (Brailov et al., 2000; Hamon et al., 1999). However, as mentioned above, the specificity of antibodies used in some of these studies was challenged by the results of *in situ* hybridization experiments. Further studies performed on primary cultured neurons overexpressing tagged versions of the receptor also indicated its ciliary localization (Berbari et al., 2008; Guadiana et al., 2013; Hu et al., 2017; Jiang et al., 2019; Kohli et al., 2017; Lesiak et al., 2018) while other studies showed a somato-dendritic localization of the receptor overexpressed in neurons (Duhr et al., 2014; Pujol et al., 2020). It has also been suggested that the receptor expression level may affect its final subcellular localization. Using a tyramide booster to enhance the GFP antibody signal, we showed in primary neurons from Htr6-GFP mice a discrete expression of the receptor in the cell body, dendrites and dendritic spines in addition to a strong ciliary expression (Chaumont-Dubel et al., 2020). Here, we showed, *in vivo* as well as in ESCs, a predominant ciliary localization in cells possessing a primary cilium. We detected 5-HT$_6$R in AC3- or ARl13b-positive cilia in the adult mouse brain, confirming that it is predominantly expressed in primary cilia in neurons and astrocytes. Using a cAMP-sensitive biosensor, Jiang et al. showed that the 5-HT$_6$R displays constitutive activity at Gs signaling only when it is expressed outside the cilium in transfected mIMCD3 cells, indicating that receptor subcellular localization strongly influences it signal transduction capacity (Jiang et al., 2019). Given the presence of 5-HT$_6$Rs exhibiting constitutive activity in adult mice brain (Deraredj Nadim et al., 2016), it is likely that a portion of the receptor is located outside the cilium in adult mouse brain. In cilia, the receptor is coupled to a Gq/11-RhoA pathway leading to actin cytoskeleton remodeling and chromatin rearrangement (Sheu et al., 2022). This latter study also demonstrated the presence of axo-ciliary synapses, which strongly suggests that ciliary receptors can be activated independently of receptors expressed in

somato-dendritic compartment. The roles of ciliary receptors *vs.* those located outside the cilium remain largely unexplored. We recently showed that 5-HT_6Rs expressed in cilia control chromatin condensation, probably through specific epigenetic modulation (Sheu et al., 2022). Activation of ciliary 5-HT_6Rs modulates nuclear actin through the activation of a Gq-RhoA-TRIO signaling pathway, which can modify global chromatin state. It also promotes histone H4K5 acetylation, thus regulating chromatin accessibility and gene expression (Sheu et al., 2022). Another example of a ciliary receptor modulating chromatin structure is the FFAR4 receptor, but its effect involves Gs and cAMP production (Hilgendorf et al., 2019). This suggests that receptors located in the primary cilium could serve as sensors of extracellular signals, that are directly connected to the nucleus.

Astrocytic cilia do not possess the same characteristics as neuronal cilia. Morphologically, they are much smaller than neuronal cilia and they are not connected to chemical synapses, the contribution of the 5-HT_6R to chromatin regulation in this cell type. Contrary to neuronal cilia, mature astrocytic cilia retain expression smoothened and Patch1, allowing for activation of the sonic hedgehog signaling (Shh) pathway (Sterpka and Chen, 2018). Previous studies have shown that stimulation of the 5-HT_6R activates the Shh pathway (Jiang et al., 2019), which could affect the proliferation of reactive astrocytes and inhibit inflammation (Allahyari et al., 2019; Sirko et al., 2013). Activation of the 5-HT_6R might therefore play a major role in these two processes. Given the importance of neuroinflammation in psychiatric disorders (Pape et al., 2019), further studies addressing the function of the 5-HT_6R in astrocytic cilia would certainly be of great interest.

Another study has shown that pharmacological inhibition of the 5-HT_6R reduces cilia length (Brodsky et al., 2017). Changes in ciliary morphology have been described in pathological situations. In mice over-expressing Arl13b, the primary cilia become longer, and the mice are prone to spontaneous seizures. Neuronal cilia get shorter in the brain under reactive insult (Sterpka et al., 2020). In the APP-PS1 model of Alzheimer's disease, the 5-HT_6R is overexpressed and primary cilia are elongated (Hu et al., 2017). Corroborating these observations, we show in the present study that neuronal cilia are shorter in Htr6-KO mice than in WT mice. Collectively, these results are consistent with the hypothesis that the receptor is an important regulator of primary cilia morphology. This suggests that it may have a significant role in cilia function, but this role is still unclear.

Given the key influence of 5-HT_6R on neurodevelopmental processes, we also sought to describe the expression pattern of the receptor during neurodevelopment. Reminiscent of our observation in adult mice, we only detected the receptor in primary cilia in embryonic brain, with a similar regional expression pattern. Notably, a strong expression of the receptor was detected in the ventricular and subventricular zones, two areas important for neurogenesis and neuronal differentiation. Intriguingly, we observed a transient relocation of 5-HT_6R from primary cilia to soma membrane in some but not all brain regions at the neonatal stage, when neuronal circuits are rearranged to establish the mature neuronal connectivity necessary for higher brain functions such as cognition. Our previous studies demonstrated that during the first post-natal week, the 5-HT_6R interacts with GPRIN1, a protein located in the soma of neurons, but not in the primary cilium (Pujol et al., 2020). Accordingly, the interaction between the two proteins occurs exclusively at the soma membrane. We also showed that this interaction potentiates the constitutive activity of the receptor towards the cAMP pathway and results in longer and more branched neurites (Pujol et al., 2020). We therefore hypothesize that 5-HT_6R relocation from primary cilia to the soma of neurons at the neonatal stage might a be a critical mechanism contributing to its role in neurite extension and maturation that underlie neuronal circuit refinement at the neonatal stage.

4. Conclusion

This study extensively characterizes the endogenous 5-HT_6R expression at the protein level in developing and adult mouse brains. It shows that the receptor regional distribution is well correlated with its role in higher cognitive functions, feeding and nociception. It also resolved the persistent conundrums of its expression in projection excitatory neurons *vs.* GABAergic interneurons, its expression in astrocytes, and its localization in primary cilium *vs.* soma plasma membrane of neurons. Finally, it reveals dynamic changes in receptor localization in neurons at the neonatal stage, which might underlie its key role in neurodevelopmental and cognitive processes.

5. Material & methods

5.1. Animals

5-$HT_6^{GFP/GFP}$ KI (Htr6-GFP) and 5-$HT_6^{-/-}$ KO mice (Htr6-KO) were generated at the Institut Clinique de la Souris (Illkirch-Graffenstaden, France) and C57BL/6 J mice originate from Janvier laboratories. Procedures were performed in strict compliance with the animal use and care guidelines of Montpellier University (Authorization D34–172-4). Both male and female mice were used.

To validate the use of the Htr6-GFP mouse line for studying the expression and subcellular localization of the 5-HT_6R, we first examined that the insertion of the GFP tag does not alter receptor function. We compared the activation of the tagged and untagged receptors by the specific agonist (WAY181,187) (Fig. S5), and detected no difference. We also previously showed that the GFP-tagged receptor can induce neurite outgrowth and neuronal differentiation in an NG108–15 neuroblastoma cell line (Duhr et al., 2014). Finally, the GFP-tagged 5-HT_6R was used in studies investigating the targeting of the receptor to the primary cilium, suggesting that this tag does not affect the proper subcellular localization of the receptor (Barbeito et al., 2021; Berbari et al., 2008). Taken together these data suggest that inserting a GFP tag does not alter 5-HT6R functionality.

5.2. Immunohistochemistry experiments

For immunohistochemistry at the adult stage, two-month-old mice were rapidly anesthetized with isoflurane and perfused transcardially with ice-cold Artificial cerebrospinal fluid (ACSF). For primary cilia length measurements, two-month-old mice were rapidly anesthetized with isoflurane and perfused transcardially with 4% PFA diluted in PBS. Brains were then postfixed in 4% PFA diluted in PBS for 24 h at 4 °C and then rinsed 3 times in PBS. Fifty μm-thick sections were cut with a vibratome (Leica) and stored at −20 °C in a cryoprotective solution (30% ethylene glycol, 30% glycerol, 25% PBS, 15% H2O) until use. For immunohistochemistry at the embryonic stage, embryos were beheaded, brains were rapidly extracted then fixed in 4% PFA diluted in PBS for 24 h at 4 °C. They were then rinsed 3 times in PBS. Embryonic brains were then incubated successively in 10, 20, and 30% (*w/v*) sucrose diluted in PBS for cryoprotection. Twenty μm-thick sections were cut with a cryostat (Leica). For immunolabeling experiments, sections were rinsed for 15 min in PBS. In order to block non-specific binding of antibodies and permeabilize the cells, sections were incubated for 2 h in PBS containing 0.2% (*v*/v) TritonX-100, 3% (w/v) bovine serum albumin (BSA; A2153, Sigma-Aldrich). They were then incubated overnight at room temperature with primary antibodies in PBS, 0.2% Triton X-100, 1% BSA. Sections were then washed three times for 30 min in PBS and incubated with Fluorophore-coupled secondary antibodies (Alexa Fluor, Life Technologies, 1/1000 dilution). Sections were washed three times for 30 min each in PBS and mounted in fluorescence mounting medium (Dako Agilent). Images of different focus points in the Z axis were acquired with a Leica SP8 confocal microscope equipped with an oil-immersed 63× objective, with a 2048 × 2048 resolution, and 0.5 μm between focus points.

List of antibodies

Species	Immunoreactivity	Dilution	Ref
Chicken	GFP	1/500	Invitrogen A10262
Rabbit	GFP	1/1000	Chromotek PABG1
Rabbit	AC3	1/5000	Universal Biological RPCA-ACIII-AP
Mouse	Arl13b	1/1000	Antibodies inc. 75–287
Mouse	S100Beta	1/500	Abcam AB11178
Rabbit	GFAP	1/1000	DAKO Z0334
Mouse	NeuN	1/500	EMD Millipore MAB337
Rabbit	GABA	1/1000	Sigma A2052
Rabbit	DARPP-32	1/1000	Cell signaling technology #2306
Rabbit	WFS-1	1/500	Proteintech 11,558–1-AP

5.3. Primary cilia counting and length measurements

Threshold was applied to the images using Image J software to define the primary cilium structure. When length was not measured, the number of primary cilia per field was determined using the particle analyzer. The number of Dapi-positive nuclei in the same field was determined in the same way. The percentage of Dapi-positive and cilia-positive cells was then calculated. To determine the cilia length, 3-D reconstructions were obtained from stacks acquired with a Leica SP8 confocal microscope equipped with an oil-immersed 63× objective, with a 2048 × 2048 resolution, and 0.5 µm between focus points. Each individual primary cilium was traced using the "Simple neurite tracer" plug-in from the Image J software.

5.4. Quantitative PCR (qPCR)

Striata of Htr6-GFP mice at different ages were collected (three animals per point). RNAs were prepared from the tissues using the Quick-RNA miniprep kit (Zymo research). 150 ng of RNA was reverse-transcribed using MMLV-RT and N6 primers (Life technologies). qPCRs were performed in triplicates in 384-well plates using SYBR Green mix (Roche), on a Light Cycler LC480 Real-Time PCR system (Roche). Three house-keeping genes (HKG) were selected using GeNorm (Vandesompele et al., 2002) (Gus, Mrlp32 and Tfrc) to normalize the expression of the Htr6 gene.

List of primers

Gene ID	Sequence forward (5′ to 3′)	Sequence reverse (3′ to 5′)
Htr6	CCTGGTGTCGCTCTTCACG	GGCATCACCACCAATCCC
Gus	GATTCAGATATCCGAGGGAAAGG	GCCAACGGAGCAGGTTGA
Mrlp32	AGGTGCTGGGAGCTGCTACA	AAAGCGACTCCAGCTCTGCT
Tfrc	AGACCTTGCACTCTTTGGACATG	GGTGTGTATGGATCACCAGTTCCTA

5.5. ES cell culture

5.5.1. Generation of a doxycycline-inducible Htr6GFP ESC line (ICE-Htr6GFP)

ICE-Inducible Cassette Exchange Recombination- A2lox.Cre mouse ESCs (Iacovino et al.) were cultivated on mitomycin-arrested mouse embryonic fibroblasts (MEFs) in ESC media. ESC media consists of DMEM supplemented with 15% fetal bovine serum, 0.1 mM non-essential amino acids, 1 mM sodium pyruvate, 50 $U.ml^{-1}$ penicillin/streptomycin (all from Life Technologies), 0.1 mM β-mercaptoethanol (Sigma), and 1000 $U.ml^{-1}$ leukemia inhibitor factor (Millipore). ESCs were changed every day with ESC media and propagated as described (Gaspard et al., 2009).

The 5htr6 mouse sequence flanked with GFP and HA tags was amplified by PCR and introduced into the p2 lox plasmid (Iacovino et al., 2011). The insert was verified by Sanger sequencing. ICE ESCs were stimulated with 1 $\mu g.ml^{-1}$doxycycline (allowing CRE induction). The next day, ICE-ESC were electroporated using a Neon system (set at 1200 V, 20 ms, and 2 pulses) with 5 µg of the p2lox-Htr6GFP plasmid. Electroporated ESCs were seeded onto Neo-resistant MEFs in ESC medium. ICE ESCs were selected with G418 (300 µg/ml). Survivor ESC clones were picked and amplified in ESC media. Clones were treated for 24 h with doxycycline (1 $\mu g.ml^{-1}$) or DMSO (vehicle, as control) and screened for GFP fluorescence.

5.5.2. Neural differentiation of ESCs

ICE-GFP cells, expressing cytosolic GFP were used as control, and grown at the same time as ICE-Htr6GFP cells. ESCs cultivated on MEFs were trypsinised. To enrich for ESCs, the MEFs-ESCs suspension was passed through a 15-µm cell trainer (Pluriselect). This pore size retains MEFs while ESCs pass through. ESCs (flow-through) were counted using a Malassez counting chamber and 1 ml of ESCs suspension (at 10,000 ESCs/ml in ESC medium) was plated on glass coverslips coated with Laminin (3 µg/ml in PBS, Becton-Dickinson) in a 12-well plate. The next day (considered as day 0 of differentiation) the ESC media was removed, ESCs were rinsed with PBS, and cultivated into corticogenesis media (adapted from (Gaspard et al., 2009)). Corticogenesis media consists of DMEM-F12 Glutamax supplemented with N2, B27 minus vitamin A, 0.1 mM non-essential amino acids solution, 500 µg/ml BSA, 1 mM sodium pyruvate, 50 $U.ml^{-1}$ penicillin and streptomycin (all from Life Technologies), 0.1 mM 2-mercaptoethanol (Sigma) and the BMP inhibitor DMH1-HCl (1 µM). The corticogenesis medium was changed every other day. Induction of the expression of the transgene was achieved using doxycycline (1 µg/ml) for 24 h. DMSO served as a no-induction control.

5.6. Immunofluorescence on ES cells

Pluripotent or differentiated ESC were grown on coverslips and fixed for 20 min in 4% paraformaldehyde. No amplification of the GFP signal was necessary for either of the cell line. Arl13b labeling (1/1000) as well as DAPI staining of the nuclei was performed (1/5000). Coverslips were washed in PBS before incubating the cells for 30 min at room temperature in a solution containing 5% serum, 3% BSA and 0.3% triton X-100 for blocking of nonspecific sites and permeabilization. Primary antibody was diluted in 1% serum, 3% BSA and 0.1% triton X-100 and incubated overnight at 4 °C. After washing 3 times in PBS, the secondary antibody was added in the same solution and left for 1 h at room temperature. Coverslips were washed twice in PBS and DAPI solution was added for 5 min at room temperature. Coverslips were washed in water and mounted on glass slides using Mowiol. Images were acquired on a Zeiss apotome microscope using an oil-immerged 63× objective.

5.7. Measurement of cAMP production in NG108–15 cells

NG108–15 cells were transfected with plasmids encoding the 5-HT_6 receptor tagged or not with GFP and grown in 24-well culture dishes in culture medium containing DMEM and 2% dialyzed Fetal Calf Serum. Twenty-four hours after transfections, culture media was removed and cells were washed in Stimulation buffer containing 140 mM NaCl, 1.2 mM KH_2PO_4, 5 mM KCl, 1.2 mM $MgSO_4$, 10 mM Glucose, 10 mM Hepes and 2 m M $CaCl_2$, pH 7.4. Cells were then exposed for 5 min at 37 °C to SB258585 a specific 5-HT_6R agonist at concentrations ranging from

10^{-9} to 10^{-7} M in 250 µl stimulation buffer containing 1 mM IBMX, before addition of 250 µl of 1% Triton X-100 and a further 30-min incubation at 37 °C. Supernatants are collected and cAMP accumulation was measured using the cAMP Gs dynamic kit (Cisbio-Perkin Elmer) according to the manufacturer's protocol. Twenty µl of each sample were transferred in a black 96 well plate and diluted in 30 µl diluent solution. Samples were incubated overnight at 4 °C with cAMP-D2 reagent and anti-cAMP cryptate (50 µl each) and the signal was read using a Rubystar plate reader.

5.8. Statistical analysis

Data was analyzed using the Graphpad Prism software, except for data on Fig. 6, which was analyzed using the estimationstats.com website. The statistical tests that were used are indicated in the figure legend.

Authors contributions

CRediT roles: Conceptualization: JB, TB, PM, SCD; Formal analysis: VD, MP, AP, CM, EV, TB, SCD; Funding acquisition: PM, SCD; Investigation VD, MP, AP, CM, EV, TB, SCD; Methodology: VD, MP, EV, JB, TB, PM, SCD; Project administration: PM, SCD; Ressources: EV, TB, PM, SCD; Supervision EV, JB, TB, PM, SCD; Validation: VD, MP, AP, CM, EV, TB, PM, SCD; Visualization: VD, MP, EV, TB, PM, SCD; writing original draft: SCD; Review and editing: EV, TB, JB, PM, SCD.

Declaration of Competing Interest

The authors declare they have no competing interests.

Data availability

Data will be made available on request.

Acknowledgements

For microscopy experiments, we acknowledge the imaging facility MRI, member of the national infrastructure France-BioImaging infrastructure supported by the French National Research Agency (ANR-10-INBS-04, «Investments for the future»). The authors thank the iExplore Facility, RAM, BioCampus. We thank Dr. Michael Kyba (University of Minnesota) for A2Lox.Cre mES cells and the p2Lox-GFP plasmid. The generation of Htr6-EGFP KI mice was supported by Foundation for Medical Research (FRM, France) and ANR contract Sero6Cognet (ANR-11-BSV4-008). Generation of Htr6 KO mice was supported by the Phenomin consortium. Funding: This study was supported by ANR grant Sero6Dev (ANR-17-CE16-0010-01), the University of Montpellier (ANR-16-IDEX-0006), CNRS and INSERM.

Appendix A. Supplementary data

Supplementary data to this article can be found online at https://doi.org/10.1016/j.nbd.2022.105949.

References

Allahyari, R.V., Clark, K.L., Shepard, K.A., Garcia, A.D.R., 2019. Sonic hedgehog signaling is negatively regulated in reactive astrocytes after forebrain stab injury. Sci. Rep. 9, 565.

Arellano, J.I., Guadiana, S.M., Breunig, J.J., Rakic, P., Sarkisian, M.R., 2012. Development and distribution of neuronal cilia in mouse neocortex. J. Comp. Neurol. 520, 848–873.

Barbeito, P., Tachibana, Y., Martin-Morales, R., Moreno, P., Mykytyn, K., Kobayashi, T., Garcia-Gonzalo, F.R., 2021. HTR6 and SSTR3 ciliary targeting relies on both IC3 loops and C-terminal tails. Life Sci. Alliance 4.

Berbari, N.F., Johnson, A.D., Lewis, J.S., Askwith, C.C., Mykytyn, K., 2008. Identification of ciliary localization sequences within the third intracellular loop of G protein-coupled receptors. Mol. Biol. Cell 19, 1540–1547.

Berthoux, C., Hamieh, A.M., Rogliardo, A., Doucet, E.L., Coudert, C., Ango, F., Grychowska, K., Chaumont-Dubel, S., Zajdel, P., Maldonado, R., Bockaert, J., Marin, P., Becamel, C., 2020. Early 5-HT6 receptor blockade prevents symptom onset in a model of adolescent cannabis abuse. EMBO Mol. Med. 12, e10605.

Brailov, I., Bancila, M., Brisorgueil, M.J., Miquel, M.C., Hamon, M., Verge, D., 2000. Localization of 5-HT(6) receptors at the plasma membrane of neuronal cilia in the rat brain. Brain Res. 872, 271–275.

Brodsky, M., Lesiak, A.J., Croicu, A., Cohenca, N., Sullivan, J.M., Neumaier, J.F., 2017. 5-HT6 receptor blockade regulates primary cilia morphology in striatal neurons. Brain Res. 1660, 10–19.

Cai, Y., Xing, L., Yang, T., Chai, R., Wang, J., Bao, J., Shen, W., Ding, S., Chen, G., 2021. The neurodevelopmental role of dopaminergic signaling in neurological disorders. Neurosci. Lett. 741, 135540.

Chaumont-Dubel, S., Dupuy, V., Bockaert, J., Becamel, C., Marin, P., 2020. The 5-HT6 receptor interactome: new insight in receptor signaling and its impact on brain physiology and pathologies. Neuropharmacology 172, 107839.

Codony, X., Vela, J.M., Ramirez, M.J., 2011. 5-HT(6) receptor and cognition. Curr. Opin. Pharmacol. 11, 94–100.

Daubert, E.A., Condron, B.G., 2010. Serotonin: a regulator of neuronal morphology and circuitry. Trends Neurosci. 33, 424–434.

Dayer, A.G., Jacobshagen, M., Chaumont-Dubel, S., Marin, P., 2015. 5-HT6 receptor: a new player controlling the development of neural circuits. ACS Chem. Neurosci. 6, 951–960.

de Bruin, N., van Loevezijn, A., Wicke, K.M., de Haan, M., Venhorst, J., Lange, J.H.M., de Groote, L., van der Neut, M.A.W., Prickaerts, J., Andriambeloson, E., Foley, A.G., van Drimmelen, M., van der Wetering, M., Kruse, C.G., 2016. The selective 5-HT6 receptor antagonist SLV has putative cognitive- and social interaction enhancing properties in rodent models of cognitive impairment. Neurobiol. Learn. Mem. 133, 100–117.

Deneris, E., Gaspar, P., 2018. Serotonin neuron development: shaping molecular and structural identities. Wiley Interdiscip. Rev. Dev. Biol. 7.

Deraredj Nadim, W., Chaumont-Dubel, S., Madouri, F., Cobret, L., De Tauzia, M.L., Zajdel, P., Benedetti, H., Marin, P., Morisset-Lopez, S., 2016. Physical interaction between neurofibromin and serotonin 5-HT6 receptor promotes receptor constitutive activity. Proc. Natl. Acad. Sci. U. S. A. 113, 12310–12315.

Doucet, E., Grychowska, K., Zajdel, P., Bockaert, J., Marin, P., Becamel, C., 2021. Blockade of serotonin 5-HT6 receptor constitutive activity alleviates cognitive deficits in a preclinical model of neurofibromatosis type 1. Int. J. Mol. Sci. 22.

Duhr, F., Deleris, P., Raynaud, F., Seveno, M., Morisset-Lopez, S., Mannoury la Cour, C., Millan, M.J., Bockaert, J., Marin, P., Chaumont-Dubel, S., 2014. Cdk5 induces constitutive activation of 5-HT6 receptors to promote neurite growth. Nat. Chem. Biol. 10, 590–597.

Ferrero, H., Solas, M., Francis, P.T., Ramirez, M.J., 2017. Serotonin 5-HT6 receptor antagonists in Alzheimer's disease: therapeutic rationale and current development status. CNS Drugs 31, 19–32.

Gaspar, P., Cases, O., Maroteaux, L., 2003. The developmental role of serotonin: news from mouse molecular genetics. Nat. Rev. Neurosci. 4, 1002–1012.

Gaspard, N., Bouschet, T., Herpoel, A., Naeije, G., van den Ameele, J., Vanderhaeghen, P., 2009. Generation of cortical neurons from mouse embryonic stem cells. Nat. Protoc. 4, 1454–1463.

Gerard, C., el Mestikawy, S., Lebrand, C., Adrien, J., Ruat, M., Traiffort, E., Hamon, M., Martres, M.P., 1996. Quantitative RT-PCR distribution of serotonin 5-HT6 receptor mRNA in the central nervous system of control or 5,7-dihydroxytryptamine-treated rats. Synapse 23, 164–173.

Gerard, C., Martres, M.P., Lefevre, K., Miquel, M.C., Verge, D., Lanfumey, L., Doucet, E., Hamon, M., el Mestikawy, S., 1997. Immuno-localization of serotonin 5-HT6 receptor-like material in the rat central nervous system. Brain Res. 746, 207–219.

Grychowska, K., Satala, G., Kos, T., Partyka, A., Colacino, E., Chaumont-Dubel, S., Bantreil, X., Wesolowska, A., Pawlowski, M., Martinez, J., Marin, P., Subra, G., Bojarski, A.J., Lamaty, F., Popik, P., Zajdel, P., 2016. Novel 1H-Pyrrolo[3,2-c]quinoline based 5-HT6 receptor antagonists with potential application for the treatment of cognitive disorders associated with Alzheimer's disease. ACS Chem. Neurosci. 7, 972–983.

Guadiana, S.M., Semple-Rowland, S., Daroszewski, D., Madorsky, I., Breunig, J.J., Mykytyn, K., Sarkisian, M.R., 2013. Arborization of dendrites by developing neocortical neurons is dependent on primary cilia and type 3 adenylyl cyclase. J. Neurosci. 33, 2626–2638.

Hamon, M., Doucet, E., Lefevre, K., Miquel, M.C., Lanfumey, L., Insausti, R., Frechilla, D., Del Rio, J., Verge, D., 1999. Antibodies and antisense oligonucleotide for probing the distribution and putative functions of central 5-HT6 receptors. Neuropsychopharmacology 21, 68S–76S.

Helboe, L., Egebjerg, J., de Jong, I.E., 2015. Distribution of serotonin receptor 5-HT6 mRNA in rat neuronal subpopulations: a double in situ hybridization study. Neuroscience 310, 442–454.

Higginbotham, H., Eom, T.Y., Mariani, L.E., Bachleda, A., Hirt, J., Gukassyan, V., Cusack, C.L., Lai, C., Caspary, T., Anton, E.S., 2012. Arl13b in primary cilia regulates the migration and placement of interneurons in the developing cerebral cortex. Dev. Cell 23, 925–938.

Hilgendorf, K.I., Johnson, C.T., Mezger, A., Rice, S.L., Norris, A.M., Demeter, J., Greenleaf, W.J., Reiter, J.F., Kopinke, D., Jackson, P.K., 2019. Omega-3 fatty acids activate ciliary FFAR4 to control adipogenesis. Cell 179 (1289–1305), e1221.

Hirst, W.D., Price, G.W., Rattray, M., Wilkin, G.P., 1997. Identification of 5-hydroxytryptamine receptors positively coupled to adenylyl cyclase in rat cultured astrocytes. Br. J. Pharmacol. 120, 509–515.
Hirst, W.D., Cheung, N.Y., Rattray, M., Price, G.W., Wilkin, G.P., 1998. Cultured astrocytes express messenger RNA for multiple serotonin receptor subtypes, without functional coupling of 5-HT1 receptor subtypes to adenylyl cyclase. Brain Res. Mol. Brain Res. 61, 90–99.
Hirst, W.D., Abrahamsen, B., Blaney, F.E., Calver, A.R., Aloj, L., Price, G.W., Medhurst, A. D., 2003. Differences in the central nervous system distribution and pharmacology of the mouse 5-hydroxytryptamine-6 receptor compared with rat and human receptors investigated by radioligand binding, site-directed mutagenesis, and molecular modeling. Mol. Pharmacol. 64, 1295–1308.
Hirst, W.D., Stean, T.O., Rogers, D.C., Sunter, D., Pugh, P., Moss, S.F., Bromidge, S.M., Riley, G., Smith, D.R., Bartlett, S., Heidbreder, C.A., Atkins, A.R., Lacroix, L.P., Dawson, L.A., Foley, A.G., Regan, C.M., Upton, N., 2006. SB-399885 is a potent, selective 5-HT6 receptor antagonist with cognitive enhancing properties in aged rat water maze and novel object recognition models. Eur. J. Pharmacol. 553, 109–119.
Ho, J., Tumkaya, T., Aryal, S., Choi, H., Claridge-Chang, A., 2019. Moving beyond P values: data analysis with estimation graphics. Nat. Methods 16, 565–566.
Hu, L., Wang, B., Zhang, Y., 2017. Serotonin 5-HT6 receptors affect cognition in a mouse model of Alzheimer's disease by regulating cilia function. Alzheimers Res. Ther. 9, 76.
Iacovino, M., Bosnakovski, D., Fey, H., Rux, D., Bajwa, G., Mahen, E., Mitanoska, A., Xu, Z., Kyba, M., 2011. Inducible cassette exchange: a rapid and efficient system enabling conditional gene expression in embryonic stem and primary cells. Stem Cells 29, 1580–1588.
Jacobshagen, M., Niquille, M., Chaumont-Dubel, S., Marin, P., Dayer, A., 2014. The serotonin 6 receptor controls neuronal migration during corticogenesis via a ligand-independent Cdk5-dependent mechanism. Development 141, 3370–3377.
Jiang, J.Y., Falcone, J.L., Curci, S., Hofer, A.M., 2019. Direct visualization of cAMP signaling in primary cilia reveals up-regulation of ciliary GPCR activity following hedgehog activation. Proc. Natl. Acad. Sci. U. S. A. 116, 12066–12071.
Jurga, A.M., Paleczna, M., Kadluczka, J., Kuter, K.Z., 2021. Beyond the GFAP-astrocyte protein markers in the brain. Biomolecules 11.
Kiprilov, E.N., Awan, A., Desprat, R., Velho, M., Clement, C.A., Byskov, A.G., Andersen, C.Y., Satir, P., Bouhassira, E.E., Christensen, S.T., Hirsch, R.E., 2008. Human embryonic stem cells in culture possess primary cilia with hedgehog signaling machinery. J. Cell Biol. 180, 897–904.
Kohen, R., Metcalf, M.A., Khan, N., Druck, T., Huebner, K., Lachowicz, J.E., Meltzer, H. Y., Sibley, D.R., Roth, B.L., Hamblin, M.W., 1996. Cloning, characterization, and chromosomal localization of a human 5-HT6 serotonin receptor. J. Neurochem. 66, 47–56.
Kohli, P., Hohne, M., Jungst, C., Bertsch, S., Ebert, L.K., Schauss, A.C., Benzing, T., Rinschen, M.M., Schermer, B., 2017. The ciliary membrane-associated proteome reveals actin-binding proteins as key components of cilia. EMBO Rep. 18, 1521–1535.
Lesiak, A.J., Brodsky, M., Cohenca, N., Croicu, A.G., Neumaier, J.F., 2018. Restoration of physiological expression of 5-HT6 receptor into the primary cilia of null mutant neurons lengthens both primary cilia and dendrites. Mol. Pharmacol. 94, 731–742.
Li, X., Gao, L., Liu, J., Zhang, H., Chen, H., Yang, L., Wu, M., Li, C., Zhu, X., Ding, Y., Sun, L., 2021. Safety, tolerability and pharmacokinetics of the serotonin 5-HT6 receptor antagonist, HEC30654, in healthy Chinese subjects. Front. Pharmacol. 12, 726536.
Martin, P.Y., Doly, S., Hamieh, A.M., Chapuy, E., Canale, V., Drop, M., Chaumont-Dubel, S., Bantreil, X., Lamaty, F., Bojarski, A.J., Zajdel, P., Eschalier, A., Marin, P., Courteix, C., 2020. mTOR activation by constitutively active serotonin6 receptors as new paradigm in neuropathic pain and its treatment. Prog. Neurobiol. 193, 101846.
Meffre, J., Chaumont-Dubel, S., Mannoury la Cour, C., Loiseau, F., Watson, D.J., Dekeyne, A., Seveno, M., Rivet, J.M., Gaven, F., Deleris, P., Herve, D., Fone, K.C., Bockaert, J., Millan, M.J., Marin, P., 2012. 5-HT(6) receptor recruitment of mTOR as a mechanism for perturbed cognition in schizophrenia. EMBO Mol. Med. 4, 1043–1056.
Monsma Jr., F.J., Shen, Y., Ward, R.P., Hamblin, M.W., Sibley, D.R., 1993. Cloning and expression of a novel serotonin receptor with high affinity for tricyclic psychotropic drugs. Mol. Pharmacol. 43, 320–327.
Morozova, M., Burminskiy, D., Rupchev, G., Lepilkina, T., Potanin, S., Beniashvili, A., Lavrovsky, Y., Vostokova, N., Ivaschenko, A., 2017. 5-HT6 receptor antagonist as an adjunct treatment targeting residual symptoms in patients with schizophrenia: unexpected sex-related effects (double-blind placebo-controlled trial). J. Clin. Psychopharmacol. 37, 169–175.
Pape, K., Tamouza, R., Leboyer, M., Zipp, F., 2019. Immunoneuropsychiatry - novel perspectives on brain disorders. Nat. Rev. Neurol. 15, 317–328.
Paridaen, J.T., Wilsch-Brauninger, M., Huttner, W.B., 2013. Asymmetric inheritance of centrosome-associated primary cilium membrane directs ciliogenesis after cell division. Cell 155, 333–344.
Pujol, C.N., Dupuy, V., Seveno, M., Runtz, L., Bockaert, J., Marin, P., Chaumont-Dubel, S., 2020. Dynamic interactions of the 5-HT6 receptor with protein partners control dendritic tree morphogenesis. Sci. Signal. 13.
Rahman, M.A., Kim, H., Lee, K.H., Yun, H.M., Hong, J.H., Kim, Y., Choo, H., Park, M., Rhim, H., 2017. 5-Hydroxytryptamine 6 receptor (5-HT6R)-mediated morphological changes via RhoA-dependent pathways. Mol. Cell 40, 495–502.
Riccio, O., Potter, G., Walzer, C., Vallet, P., Szabo, G., Vutskits, L., Kiss, J.Z., Dayer, A.G., 2009. Excess of serotonin affects embryonic interneuron migration through activation of the serotonin receptor 6. Mol. Psychiatry 14, 280–290.
Ruat, M., Traiffort, E., Arrang, J.M., Tardivel-Lacombe, J., Diaz, J., Leurs, R., Schwartz, J. C., 1993. A novel rat serotonin (5-HT6) receptor: molecular cloning, localization and stimulation of cAMP accumulation. Biochem. Biophys. Res. Commun. 193, 268–276.
Sarkisian, M.R., Guadiana, S.M., 2015. Influences of primary cilia on cortical morphogenesis and neuronal subtype maturation. Neuroscientist 21, 136–151.
Sheu, S.H., Upadhyayula, S., Dupuy, V., Pang, S., Deng, F., Wan, J., Walpita, D., Pasolli, H.A., Houser, J., Sanchez-Martinez, S., Brauchi, S.E., Banala, S., Freeman, M., Xu, C.S., Kirchhausen, T., Hess, H.F., Lavis, L., Li, Y., Chaumont-Dubel, S., Clapham, D.E., 2022. A serotonergic axon-cilium synapse drives nuclear signaling to alter chromatin accessibility. Cell 185 (3390–3407), e3318.
Sipos, E., Komoly, S., Acs, P., 2018. Quantitative comparison of primary cilia marker expression and length in the mouse brain. J. Mol. Neurosci. 64, 397–409.
Sirko, S., Behrendt, G., Johansson, P.A., Tripathi, P., Costa, M., Bek, S., Heinrich, C., Tiedt, S., Colak, D., Dichgans, M., Fischer, I.R., Plesnila, N., Staufenbiel, M., Haass, C., Snapyan, M., Saghatelyan, A., Tsai, L.H., Fischer, A., Grobe, K., Dimou, L., Gotz, M., 2013. Reactive glia in the injured brain acquire stem cell properties in response to sonic hedgehog. [corrected]. Cell Stem Cell 12, 426–439.
Sterpka, A., Chen, X., 2018. Neuronal and astrocytic primary cilia in the mature brain. Pharmacol. Res. 137, 114–121.
Sterpka, A., Yang, J., Strobel, M., Zhou, Y., Pauplis, C., Chen, X., 2020. Diverged morphology changes of astrocytic and neuronal primary cilia under reactive insults. Mol. Brain 13, 28.
Tang, X., Jaenisch, R., Sur, M., 2021. The role of GABAergic signalling in neurodevelopmental disorders. Nat. Rev. Neurosci. 22, 290–307.
Vanda, D., Soural, M., Canale, V., Chaumont-Dubel, S., Satala, G., Kos, T., Funk, P., Fulopova, V., Lemrova, B., Koczurkiewicz, P., Pekala, E., Bojarski, A.J., Popik, P., Marin, P., Zajdel, P., 2018. Novel non-sulfonamide 5-HT6 receptor partial inverse agonist in a group of imidazo[4,5-b]pyridines with cognition enhancing properties. Eur. J. Med. Chem. 144, 716–729.
Vandesompele, J., De Preter, K., Pattyn, F., Poppe, B., Van Roy, N., De Paepe, A., Speleman, F., 2002. Accurate normalization of real-time quantitative RT-PCR data by geometric averaging of multiple internal control genes. Genome Biol. 3. RESEARCH0034.
Wilkinson, D., Windfeld, K., Colding-Jorgensen, E., 2014. Safety and efficacy of idalopirdine, a 5-HT6 receptor antagonist, in patients with moderate Alzheimer's disease (LADDER): a randomised, double-blind, placebo-controlled phase 2 trial. Lancet Neurol. 13, 1092–1099.
Yoshioka, M., Matsumoto, M., Togashi, H., Mori, K., Saito, H., 1998. Central distribution and function of 5-HT6 receptor subtype in the rat brain. Life Sci. 62, 1473–1477.